Chemosphere 306 (2022) 135544

Contents lists available at ScienceDirect

Chemosphere

journal homepage: www.elsevier.com/locate/chemosphere

Zero-valent iron is not always effective in enhancing anaerobic digestion performance

Ziyin Ai [a], Sichao Zheng [a], Dan Liu [a], Siyuan Wang [a], Hongqin Wang [a], Wenli Huang [b], Zhongfang Lei [c], Zhenya Zhang [c], Fei Yang [a], Weiwei Huang [a,*]

[a] Key Laboratory of Agro-Forestry Environmental Processes and Ecological Regulation of Hainan Province, College of Ecology and Environment, Hainan University, 58 Renmin Avenue, Meilan District, Haikou, 570228, China
[b] MOE Key Laboratory of Pollution Process and Environmental Criteria, College of Environmental Science and Engineering, Nankai University, No. 94 Weijin Road, Nankai District, Tianjin, 300071, China
[c] Graduate School of Life and Environmental Sciences, University of Tsukuba, 1-1-1 Tennodai, Tsukuba, Ibaraki, 305-8572, Japan

HIGHLIGHTS

- Liquid nitrogen was applied to improve ZVI utilization efficiency during AD of SM.
- ZVI/LZVI did not affect CH_4 yield and archaeal distribution in healthy digesters.
- ZVI could alter metabolisms and activate microbes to overcome AD inhibition.
- Liquid nitrogen soaking strengthened ZVI's enhancement effect at high TAN stress.
- ZVI showed potentials in process revival.

GRAPHICAL ABSTRACT

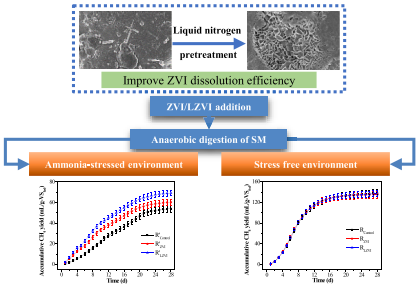

ARTICLE INFO

Handling Editor: Y Liu

Keywords:
Methane
Anaerobic digestion
Zero-valent iron
Liquid nitrogen pretreatment
Swine manure

ABSTRACT

Liquid nitrogen was employed as a low-temperature medium to activate zero-valent iron (ZVI) powder in an attempt to strengthen its enhancement effect on anaerobic digestion (AD) of swine manure (SM). Surprisingly, it was found that both pristine ZVI and liquid nitrogen-pretreated ZVI (LZVI) did not significantly improve the AD performance or change the archaeal community structure. It was hypothesized that ZVI might not be effective at stress-free environment like in these digesters. To confirm this, an additional set of AD experiments were performed at high ammonia stress (about 4000 mg/L), results showed that ZVI and LZVI greatly alleviated ammonia inhibition and increased the CH_4 yield by 11.6% and 28.2%, respectively. Apparently, ZVI mainly affected AD systems by changing the metabolism pathways and enhancing the microbial activity to overcome process inhibition, and pretreatment of liquid nitrogen could significantly accelerate the dissolution of ZVI and improve its utilization efficiency, contributing to a greater extend of process recovery and improvement.

* Corresponding author.
E-mail address: huang05106114@163.com (W. Huang).

https://doi.org/10.1016/j.chemosphere.2022.135544
Received 25 February 2022; Received in revised form 23 June 2022; Accepted 26 June 2022
Available online 30 June 2022

1. Introduction

Anaerobic digestion (AD) is a mainstream technique for swine manure (SM) stabilization. But the insufficient biogas yield still vastly restricts the commercial application of this technique (Kong et al., 2021). Generally, the CH_4 yield from SM varies within a wide range of 11–400 mL/g-VS_{fed}, depending on the source of substrate and the reaction conditions including temperature, water content, inocula ratio, pretreatment methods and toxicant concentrations (Huang et al., 2019a; Meng et al., 2020). The need to improve operability and economic feasibility of commercial AD plants has raised great interest on the development of process enhancement methods. Among them, the supplementation of zero-valent iron (ZVI) has shown great potentials in improving AD performance (Hu et al., 2020). Iron is an essential element for many anaerobic microbes (Thanh et al., 2016), and ZVI supplementation has been reported to benefit the key enzymatic reactions during AD (Yan et al., 2020). Also, ZVI dissolution has been found to efficiently reduce the unfavorable propionate-type fermentation (Yang et al., 2018), and the releasing H_2 can stimulate the activities of H_2-utilizing microorganisms to boost CH_4 generation (Wu et al., 2015). Recently, it was reported that nanoscale ZVI (nZVI) could promote direct interspecies electron transfer (DIET) between syntrophic bacteria and methanogens during AD process (Chen et al., 2020; Zhang et al., 2021).

The dissolution efficiency of ZVI is the key factor affecting its improvement effect on AD. Generally, scrap ZVI show a low reactivity because of its low surface to volume ratio (Guan et al., 2015). To guarantee adequate process performance, a high ZVI dosage is necessary. An optimal dosage of scrap ZVI as high as 50 g/L was reported by Charalambous and Vyrides (2021) when treating cheese whey using AD technology. Excess amounts of ZVI not only leads to higher chemical costs, but also represent a burden to the surrounding environment. In comparison, nZVI shows a much higher reactivity owing to its large specific surface area, and has been promptly studied for improving AD performance (Suanon et al., 2017). It was demonstrated that anaerobic microbes can directly accept electrons from nZVI to support CO_2 reduction, in addition to using H_2 as an electron donor (Tang et al., 2019). But nZVI tends to stick to the microbe cell surface and induce a negative effect on the membrane functions (Summer et al., 2020). Besides, the synthesis, storage and transportation of nZVI are very costly, making the application of nZVI in real AD plants economically infeasible. From the viewpoint of practicability, the application of micro-sized ZVI (mZVI) particles is beneficial. But a relatively high dose of mZVI is still needed due to its relatively low reactivity. Meng et al. (2020) suggested an mZVI dosage of 17.9 g/L during high-solid AD of SM. To further increase the material utilization efficiency, it is crucial to find green and cost-effective strategies to promote ZVI dissolution.

To increase the ZVI dissolution efficiency, different innovative methods including dosing ferrous ions, adding oxidants (e.g., H_2O_2, $KMnO_4$, NaClO), sulfidation pretreatment and use of weak magnetic field have been studied. Ferrous ion has been reported to facilitate the transformation of surface passivation products to magnetite and thus improve the reduction reactivity of ZVI (Tang et al., 2016). Nevertheless, it may cause a relatively low pH level which is unfavorable for AD. Despite the efficacy of chemical oxidants in facilitating ZVI corrosion, they seem not very effective in neutral or alkaline pH conditions, and the cost of oxidants is high (Rezaei and Vione, 2018). The chemical cost of sulfidation pretreatment is low, but the ball-milling process for S-ZVI synthesis is energy-intense (Fan et al., 2019). As for the use of weak magnetic field, the design of reasonable reactors is a big challenge, and the investment cost of providing stable weak magnetic field needs to be well considered (Huang et al., 2019b).

Recently, the application of liquid nitrogen as a low-temperature medium to accelerate ZVI dissolution has attracted a great deal of attentions. Liquid nitrogen is an inexpensive and nontoxic medium, it can induce a drastic temperature drop and crack the surface oxide shell of ZVI to generate micro-fractures, which increases the reactivity of ZVI (Hu et al., 2019). Compared with other pretreatment methods, soaking of liquid nitrogen is a simple, effective, energy-free and environmentally friendly option. Although the efficacy of liquid nitrogen pretreatment on improving ZVI reactivity for direct removal of contaminants from water during environmental remediation has been extensively studied, very few research has tried to employ this pretreatment strategy to activate ZVI and increase its utilization efficiency in AD systems treating SM. Liquid nitrogen pretreatment may cause a rapid release of H_2 from ZVI, which could pose an inhibitory effect on acetate degradation and hydrogenotrophic methanogenesis (Cazier et al., 2019). There is a great need for systematic study of the feasibility of liquid nitrogen pretreatment strategy, in order to provide theoretical supports for the development of efficient ZVI-based AD systems.

In this study, the feasibility of liquid nitrogen pretreatment for improving ZVI powder dissolution efficiency and strengthening its enhancement effect on CH_4 yield from SM has been investigated. The effects of pristine and pretreated ZVI on methane yield were elucidated. Microbial community structures (bacteria and archaea) of the digestate were also characterized to explore the mechanisms of liquid nitrogen-pretreated ZVI on the AD process. The results from this work are expected to provide scientific data for the sound reclamation of animal manure in practice.

Table 1
Characteristics of the raw materials.

Parameter	Raw swine manure (SM)	Inocula	Mixture
Total solids (TS, g/L)	191.7 (±5.3)	62.4 (±1.5)	75.3 (±3.1)
Volatile solids (VS, g/L)	159.5 (±2.6)	42.1 (±2.3)	60.7 (±3.1)
Total alkalinity (TA, mg/L as $CaCO_3$)	6112.9 (±81.3)	2853.5 (±59.0)	2599.9 (±140.7)
Total ammonia nitrogen (TAN, mg/L)	485.5 (±28.5)	3840.4 (±27.3)	387.0 (±27.2)
Soluble chemical oxygen demand (sCOD, mg/L)	8373.0 (±249.9)	11629.5 (±608.5)	3687.6 (±518.0)
Soluble carbohydrates (mg/L)	472.1 (±32.9)	757.3 (±53.6)	185.5 (±13.0)
Soluble proteins (mg/L)	709.6 (±24.9)	2526.3 (±109.8)	948.8 (±30.5)
Total volatile fatty acids (TVFAs, mg/L)	5726.3 (±79.6)	331.5 (±19.8)	2779.0 (±192.9)
Acetic acid (HAc, mg/L)	666.4 (±19.5)	6.1 (±0.3)	291.5 (±38.6)
Propionic acid (HPr, mg/L)	4122.8 (±183.5)	13.7 (±1.2)	1474.1 (±96.5)
iso-butyric acid (iso-HBu, mg/L)	526.6 (±14.7)	64.8 (±2.1)	197.7 (±7.1)
n-butyric acid (n-HBu, mg/L)	124.6 (±5.8)	39.2 (±0.5)	257.6 (±12.9)
iso-valeric acid (iso-HVa, mg/L)	86.7 (±2.9)	77.6 (±1.2)	268.9 (±18.7)
n-valeric acid (n-HVa, mg/L)	199.1 (±16.6)	130.1 (±5.6)	289.2 (±18.7)
Total soluble iron (mg/L)	6.4 (±0.2)	30.5 (±0.4)	4.0 (±0.3)
pH	7.9 (±0.1)	6.7 (±0.1)	7.4 (±0.1)

*All results in the table are presented as mean values of five determination ± standard deviation.

2. Materials and methods

2.1. Materials and chemicals

Raw SM was sampled from a swine house in suburban area (Haikou, China), and was stored at −20 °C. And it was defrosted at 4 °C prior to the experiment. Digestate from a batch digester (8 L) fed with SM was employed as inocula. The digester was incubated at 35 °C for 65 days in the lab to ensure complete consumption of the organic substrates. The biogas produced from this inocula during the subsequent experiments was negligible. Basic parameters of the raw materials were tested based on five repeated analysis (Table 1). Commercial ZVI powder (1–10 μm in

diameter, Fe content >99%, BET surface area 0.71 m^2/g) was purchased from a local supplier (Xindun Company, China). All reagents (analytical grade) were purchased from Macklin Company (China).

2.2. Experiments

Liquid nitrogen activation of ZVI was conducted in a Dewar flask under atmospheric environment and ambient temperature. Specifically, 30 g of ZVI powder was soaked in 300 mL of liquid nitrogen for 40 min. After that, the remaining liquid nitrogen was decanted for repeat use, and the resulting solid was dried in the oven at 60 °C for 20 h. The pretreated ZVI powder was denoted as LZVI. A field emission scanning electron microcopy (GeminiSEM 500, ZEISS, Germany) was used to characterize the surface morphologies of pristine ZVI and LZVI, and the results are demonstrated in Figure S1. As shown, liquid nitrogen pretreatment led to numerous micro-fractures in the LZVI surface, enlarging its reactive surface area. This observation was consistent with the results obtained by Hu et al. (2019).

To guarantee homogeneity of the substrate in each AD reactor, raw SM, fresh inocula and deionized water were mixed thoroughly in a 12-L container at a mass ratio of 1:1:0.7 (wet weight based). The total solids (TS) of the mixture was about 75.3 g/L (7.53%). A TS content between 5 and 10% was commonly used during AD of SM (Huang et al., 2019b; Zhang et al., 2021). And the food-to-microorganisms ratio of the mixture was 3.9 based on volatile solids (VS), this ratio was chosen according to the previous work (Yang et al., 2018). Basic characteristics of the mixture of SM and inocula were also listed in Table 1. A series of 1.5 L conical glass flasks were employed as the AD reactors. Each flask was equipped with a gas vent that connected to a 2 L gas collecting bag (E-Swich, China) and a liquid outlet for digestate sampling. Each flask was loaded with 1000 g of the well mixed substrate, and three groups of AD reactors were prepared: $R_{Control}$ without any additive; R_{ZVI} added with 5 g of pristine ZVI power and R_{LZVI} added with 5 g of LZVI powder. A ZVI dosage of 5 g/L was used based on the previous works (Yang et al., 2018; Huang et al., 2019b, 2019c). After bubbling the medium and the headspace with N_2 for 5 min, the flasks were capped with rubber stoppers and placed in a thermostatic incubator at 35 °C. Each group of AD experiment were conducted in triplicate. During 28 days' incubation, the flasks were shaken by hand for 3 min each day. Biogas volumes and compositions were analyzed at the same time every day, and liquid samples were taken periodically soon after the shaking.

To study the effects of ZVI and LZVI on AD of SM under high ammonia stress, three AD runs were performed. Specifically, raw SM, fresh inocula and deionized water were mixed thoroughly at a mass ratio of 1:1:0.7 (wet weight based), and NH_4Cl was added to the mixture to raise the total ammonia nitrogen (TAN) concentration to an inhibitory level of about 4000 mg/L (Yu et al., 2020). Then three groups of AD reactors were prepared: $R'_{Control}$ was loaded with 1000 g mixture; R'_{ZVI} was loaded with 1000 g mixture +5 g of pristine ZVI power and R_{LZVI} was loaded with 1000 g mixture +5 g of LZVI powder. Other experimental procedures were identical to the AD experiments described above.

2.3. Analytical methods

Biogas samples were quantified for volume using water displacement method. Compositions of CH_4, H_2 and CO_2 in the biogas were analyzed using an Angilent 5890-TCD gas chromatograph (US) packed with RT-Q-BOND PLOT column, the column temperature was set at 60 °C and the detector was set at 220 °C, N_2 (purity >99.999%) was used as carrier gas.

The concentrations of TS and VS were measured following the Standard Methods (APHA, 2012). And the weight of additives was calibrated. Solution pH was measured using a portable pH meter (AS600, ASONE, Japan). Total alkalinity (TA) concentration was determined using titration method using HCl solution (0.01 mol/L) to pH 4.3 with the assistance of a pH meter.

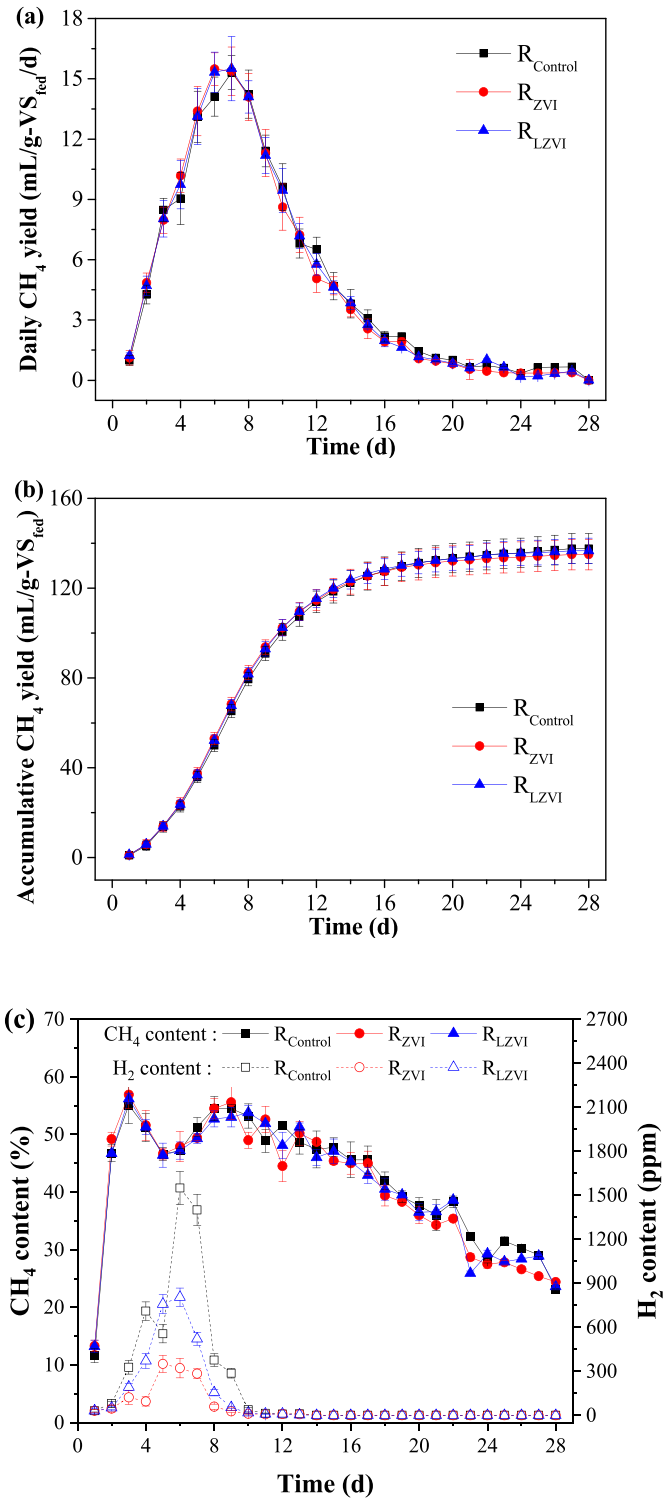

Fig. 1. Performance of (a) daily and (b) accumulative CH_4 production, variations of (c) CH_4 and H_2 content in the biogas during AD at stress-free environment.

Prior to the measurement of soluble products, the liquid samples were centrifuged at 9500 rpm for 30 min, and the supernatants were filtered through a 0.45 μm membrane. Soluble chemical oxygen demand (sCOD) and TAN were measured according to standard methods (APHA, 2012). Soluble proteins and carbohydrates were measured according to the procedures describe by Jiang et al. (2011) and Dubois et al. (1956),

respectively. Total soluble iron was measured by spectrophotometric method according to standard method 3500-Fe (APHA, 2012). The concentrations of volatile fatty acids (VFAs) were determined using an Angilent 6890-FID gas chromatograph (US) packed with an Rtx®Wax column (30 m, 0.25 mm I.D., 0.25 μm). The detector temperature was set at 200 °C and the column temperature was programmed at a rising speed of 8 °C/s from 80 to 180 °C, N_2 (purity >99.999%) was applied as the carrier gas.

2.4. Calculation

It was reported that the fraction of free ammonia nitrogen (FAN) relative to TAN is dependent on temperature (K) and pH, as illustrated in the following equation (Jiang et al., 2019).

$$FAN = TAN \times \left(1 + \frac{10^{-pH}}{10^{-\left(0.09018 + \frac{2729.92}{T}\right)}}\right)^{-1} \quad \text{(Eq 1)}$$

2.5. Microbial analysis

Liquid samples collected from different reactors after 18 days of AD were analyzed by high-throughput 16S rRNA gene pyrosequencing on the Illumuna Miseq platform (US). Detailed procedures of DNA extraction, PCR and sequencing were described in previous research (Huang et al., 2019b). Operational taxonomic units (OTUs) were defined by clustering sequences at a similarity of >97%.

2.6. Statistical analysis

Statistics obtained from the repeated experiments were analyzed by using Excel 2016 (Microsoft, USA), and "$p < 0.05$" was considered as statistical criterion.

3. Results and discussion

3.1. Biogas production

Fig. 1(a) demonstrates the daily CH_4 yield in $R_{Control}$, R_{ZVI} and R_{LZVI}. Note that the variation trends of daily CH_4 yield in the three reactors showed high similarity, increased rapidly during the initial 7 days and then declined gradually with AD time. The greatest amount of daily CH_4 yield was recorded at 15.3, 15.4 and 15.5 mL/g-VS_{fed} in $R_{Control}$, R_{ZVI} and R_{LZVI} on day 7, respectively. As exhibited in Fig. 1(b), the accumulative CH_4 yield increased gradually during day 1–19 and leveled off afterwards for all reactors. After 28 days' AD, the accumulative CH_4 yield was 137.7, 135.0 and 136.7 mL/g-VS_{fed} in $R_{Control}$, R_{ZVI} and R_{LZVI}, respectively. Surprisingly, no significant difference in the CH_4 yield was observed among the three reactors. The addition of ZVI and LZVI did not seem to significantly improve the AD performance. This observation was different from the results obtained by other authors, who reported the improvement effect of ZVI on AD performance. Shao et al. (2021) indicated that ZVI could alleviate the inhibition of chlorine disinfectants during mesophilic AD of SM and improved CH_4 yield. According to Kong et al. (2016), ZVI could eliminate excessive acidification during AD of food waste (FW) through promoting butyric acids (HBu) degradation. Yang et al. (2018) employed ZVI for alleviating ammonia inhibition during AD of SM, and the authors suggested that the presence of ZVI could facilitate the growth of ammonia-tolerant and fast-growing hydrogenotrophic *Methanoculleus*, contributing to a higher CH_4 yield by 54.2%. Huang et al. (2019c) studied the effects of ZVI on AD of SM at a high sulfadiazine concentration of 200 mg/L, and they reported that ZVI could significantly increase the overall abundance of hydrogenotrophic methanogens and contributed to a 36.9% higher CH_4 production efficiency as well as a 23.8% greater VS degradation efficiency. Pan et al. (2021) investigated the effect of nZVI/ZVI on AD systems treating toxic phenol wastewater, and the authors reported that nZVI/ZVI mainly enhanced the DIET between *Clostridium sensu stricto* and *Methanothrix*, increasing the CH_4 yield by about 23%. It was worth noting that many of these previous experiments were performed under stressed environment (i.e., high ammonia/VFAs/antibiotic/phenol concentrations, high TS or high organic loading rates). It was reasonable to deduce that the improvement effect of ZVI on methanogenesis of SM could only be significant under stressed environment. In this study, the insignificant effect of ZVI on CH_4 yield treating SM might be explained by the fact that all the three reactors were operated under stress-free environment (TS = 75.3 g/L, initial TAN = 387.0 mg/L).

Interestingly, the above hypothesis was contradictory to the study by Yan et al. (2020), who suggested that nZVI could enhance CH_4 production from sludge by acting as an intracellular electron shuttle to promote the DIET at a low ammonia load (initial TAN = 487 mg/L), and there were reasons for these seemingly inconsistent results. The effects of ZVI-induced DIET on methanogenesis performance vary depending on operational conditions like hydraulic conditions, substrate types and chemical compositions of ZVI (Inaba et al., 2019; Chen et al., 2020; Li et al., 2021; Zheng et al., 2022). After carefully reviewing the literatures, Li et al. (2021) concluded that the application of DIET in AD is substrate-dependent, simple organic acids and alcohols are preferred by electron-donating bacteria that mediating DIET, although several studies have successfully established DIET using sludge. Chen et al. (2020) have investigated the effects of mZVI and sulfidated mZVI (S-mZVI) on AD systems treating sludge and FW. According to their results, the enhancement mechanisms of S-mZVI and mZVI for CH_4 production were quite different: S-mZVI promoted the DIET between bacteria and methanogens, but had negligible effect on the hydrolysis and acidification processes; mZVI mainly promote the hydrolysis/acidification/acetogenesis process to decrease VFAs accumulation and enrich the H_2-consuming microorganisms, but no direct evidence of DIET was observed. A recent study by Inaba et al. (2019) found that nanoscale metal-based material did not promote DIET in agitated cultures, because under agitating conditions, the methanogens was unable to make close contact with the syntrophic bacteria using the conductive particles adhered or partially incorporated onto the microbial cells. In this study, no evidence was found to suggest that DIET was established with the supplementation of ZVI/LZVI, which might be attributed to the mixing condition (all reactors were shaken manually every day), used of complex organic substrate (SM) that was not preferred by DIET-related microbes, etc. The role of ZVI on the establishment of DIET during AD of animal manure and the contribution of DIET on CH_4 production should be further investigated in future studies.

Fig. 1(c) demonstrates the changes in CH_4 and H_2 contents in $R_{Control}$, R_{ZVI} and R_{LZVI}. As indicated, the CH_4 content increased quickly to a maximum of 55.1%, 56.9% and 56.2% for $R_{Control}$, R_{ZVI} and R_{LZVI} on day 3, suggesting the quick adaptation of microorganisms to achieve high methanogenesis reactivity. After a slight decline to 46.4%–46.6%, the CH_4 content again hit the top at 53.0%–55.6% on day 9 and decreased gradually afterwards. Apparently, the addition of ZVI and LZVI did not show significant impacts on the CH_4 content, this result was consistent with the daily CH_4 yield and accumulative CH_4 yield results presented above. H_2 content is also an important indicator during the AD process, low H_2 partial pressure is conducive to the spontaneous thermodynamics of the anaerobic oxidation reaction of organic acids (Feng et al., 2014). In $R_{Control}$, the H_2 content experienced a rapid rise at the beginning of AD, attaining a maximum of 1549 ppm on day 6, and it decreased gradually afterwards. The variation trends of H_2 content in R_{ZVI} and R_{LZVI} were quite similar, increased respectively to a maximum of 350 ppm on day 5 and 805 ppm on day 6, and then decreased gradually and became undetectable after day 10. Apparently, the supplementation of ZVI greatly lowered the H_2 content in the digesters. This was consistent with the previous works (Yang et al., 2018; Huang et al., 2019b), which indicated that ZVI dissolution could release H_2 to promote the growth of H_2 scavenging microorganisms, which in turn accelerated the consumption of H_2 in digester headspace and created a thermodynamically

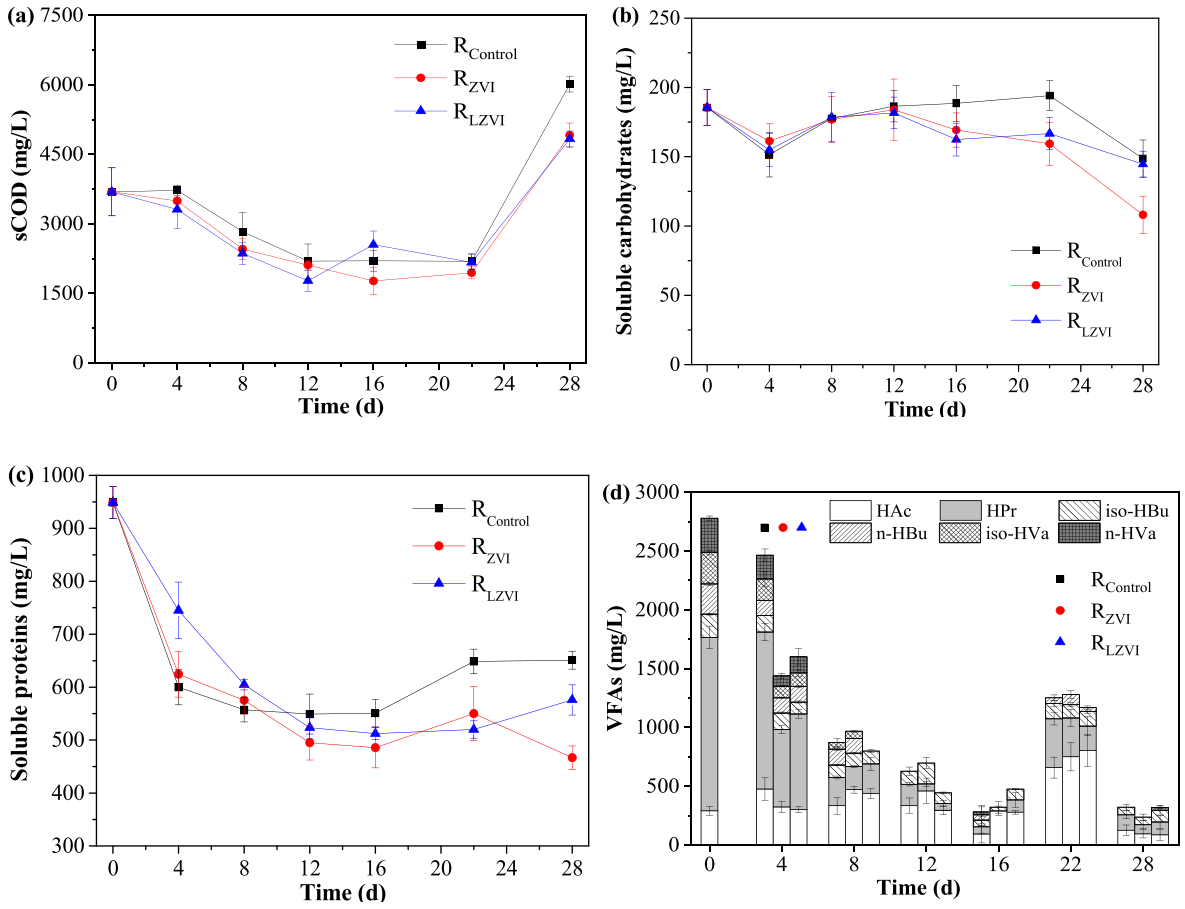

Fig. 2. Variations of (a) sCOD, (b) soluble carbohydrates, (c) soluble proteins and (d) VFAs in stress-free AD systems. HAc: acetic acid, HPr: propionic acid, iso-HBu: iso-butyric acid, n-HBu: n-butyric acid, iso-HVa: iso valeric acid, n-HVa: n-valeric a.

favorable environment to drive organic manure degradation. The relatively higher level of H_2 content in R_{LZVI} than that in R_{ZVI} was attributable to the much more efficient dissolution of LZVI after treatment by liquid nitrogen (Figure S1). It was noteworthy that despite the effectiveness of ZVI and LZVI on maintaining a much lower H_2 content in the digesters' headspace, the CH_4 yield efficiency were not affected by ZVI/LZVI addition in this study. One possible explanation was that in healthily functioning AD reactors, H_2 content was not a crucial factor for the biogasification performance. This assumption was partly supported by the rapid depletion of H_2 in all of the three reactors within 10 days' AD, which indicated the systems' capability of maintaining a good process balance.

After 28 days' AD, the removal efficiencies of TS were calculated to be 32.3% in $R_{Control}$, 28.8% in R_{ZVI} and 27.4% in R_{LZVI}. And the VS removal efficiencies were 32.9% ($R_{Control}$), 33.4% (R_{ZVI}) and 32.8% (R_{LZVI}), respectively. Overall, there was no significant difference in TS or VS removal efficiency among the three digesters, suggesting that the anaerobic biodegradability of SM was not significantly affected by the addition of ZVI/LZVI. These results agreed with our previous hypothesis that the improvement effect of ZVI on methanogenesis performance was insignificant under stress-free environment.

To verify our viewpoint, an additional set of AD experiments were conducted under high ammonia stress (TAN concentration about 4000 mg/L), and the biogas production results are presented in Figure S2 (supplementary data). As shown in Figure S2(a), the accumulative CH_4 yield from $R'_{Control}$ (54.0 mL/g-VS_{fed}) was much lower than that from $R_{Control}$ (137.7 mL/g-VS_{fed}), suggesting that the process performance was vastly hampered by the high ammonia load. The accumulative CH_4 yield from R'_{ZVI} and R'_{LZVI} on day 28 were 60.3 and 69.3 mL/g-VS_{fed}, respectively, which were 11.6% and 28.2% higher than that from $R'_{Control}$. As expected, the existence of ZVI markedly improved the CH_4 production from SM, and LZVI showed a 2.3-fold greater improvement effect than ZVI due most probably to its higher dissolution efficiency as a result of surface cracking by liquid nitrogen pretreatment. Figure S2(b) shows the variations of CH_4 and H_2 contents. It could be observed that the CH_4 content in the three reactors followed an order of $R'_{LZVI} > R'_{ZVI} > R'_{Control}$. This was in line with the experimental results obtained by many researchers (Wu et al., 2015; Kong et al., 2016; Huang et al., 2019b), in which the positive role of ZVI corrosion in promoting CO_2 reduction to CH_4 through consolidating the hydrogenotrophic methanogenesis pathway has been demonstrated. The H_2 content results were also quite different from those obtained under stress-free environment in this work. On day 1, high levels of H_2 content in the range of 620–670 ppm were detected from the three reactors, suggesting that the reactors were operated at a thermodynamically unfavorable environment due to ammonia inhibition. In $R'_{Control}$, the H_2 content varied between 260 and 620 ppm during day 1–8, then it soared to a maximum of 1240 ppm on day 11, followed by a gradual drop to become undetectable after day 18. The H_2 content in R'_{ZVI} was much lower than that in $R'_{Control}$, it fluctuated between 350 and 670 ppm during day 1–9, and slowly decreased to zero by day 18. The variation trend in R'_{LZVI} bear some resemblance to that in R'_{ZVI}, but the H_2 content was slightly higher during day 5–9, after day 9 it dropped significantly to a lower level than R'_{ZVI} due possibly to the greater effect of LZVI on regulating the H_2 scavenging processes. What noteworthy was that the three reactors operated under high ammonia concentration took much longer time (18 days) than those operated under stress-free environment (10 days) to achieve a low and nearly undetectable H_2 content, suggesting a longer time period of process imbalance as a result of ammonia inhibition. During this period, ZVI played a key role in maintaining a low H_2 environment to drive the

degradation of organic manure and overcome process inhibition (Yan et al., 2020), and liquid nitrogen pretreatment could activate ZVI and improve its utilization efficiency during AD. Nevertheless, ZVI/LZVI might not be effective for healthily functioning AD systems treating SM under stress-free environment.

To better understand the role of ZVI and LZVI in AD systems operated under stress-free environment, the changes of intermediate parameters and microbial community structures in $R_{Control}$, R_{ZVI} and R_{LZVI} were studied and discussed in the following chapters. Process results obtained during AD at ammonia-stressed environment are also provided in supplementary data for comparative analysis.

3.2. Soluble organic products

Fig. 2 illustrates the variations of soluble organic products in $R_{Control}$, R_{ZVI} and R_{LZVI}. As indicated in Fig. 2(a), the trends of sCOD in different digesters were quite similar, decreased gradually during day 0–22, followed by a rapid increase by day 28. Overall, the sCOD concentration in $R_{Control}$ was higher than those in R_{ZVI} and R_{LZVI}. On day 28, the sCOD concentrations in $R_{Control}$, R_{ZVI} and R_{LZVI} were determined to be 6013.7, 4908.7 and 4829.7 mg/L, respectively. Noted that at the end of the AD process, the concentrations of sCOD in the three reactors were higher than the initial concentrations. Contributors of sCOD includes soluble proteins, soluble carbohydrates, lipids, humic substances, long-chain and short-chain fatty acids, amino acids and other reducing substances. And the concentrations of sCOD were determined by the balance between solid hydrolysis and organic degradation through acidification/methanogenesis. The increase of sCOD at the end of the experiment might be explained by the accumulation of humic substances, which were difficult to be utilized by microorganisms. According to Cao et al. (2013), the concentrations of humic substances increased after mesophilic AD of swine and diary manure. Wang et al. (2021) also indicated an increase of humic-like components after AD of chicken manure.

As shown in Fig. 2(b), the concentrations of soluble carbohydrates in the three reactors were quite similar during day 0–12. After day 12, the level of soluble carbohydrates in R_{ZVI} and R_{LZVI} become lower than that in $R_{Control}$. According to Fig. 2(c), the concentrations of soluble proteins were greatly higher than those of soluble carbohydrates for all reactors. Similar to the trends of soluble carbohydrates, R_{ZVI} and R_{LZVI} achieved a lower level of soluble carbohydrates since day 12. These were in line with the results obtained by Huang et al. (2019b), who indicated that ZVI can accelerate the conversion of soluble proteins/carbohydrates during acidification and contribute to a lower level of these organic products in the digesters.

Fig. 2(d) depicts the changes of VFAs. In the early stage of AD, the concentrations of propionic acid (HPr) in R_{ZVI} and R_{LZVI} were significantly lower than those in $R_{Control}$. HPr is an undesirable intermediate for methanogenesis because its conversion to acetate is unfavorable in thermodynamics (Wei et al., 2018). On day 4, a relatively higher HPr concentration of 1335.6 mg/L was observed in $R_{Control}$, in comparison to that of 658.9 mg/L in R_{ZVI} and 814.0 mg/L in R_{LZVI}. After a short period of adaptation, the HPr concentration in $R_{Control}$ decreased quickly to 240.4 mg/L by day 8, which was quite close to those in R_{ZVI} (197.2 mg/L) and R_{LZVI} (252.2 mg/L), indicating that $R_{Control}$ had successfully adjusted itself to achieve process balance. This result was consistent with the H_2 content results shown in Fig. 2(c), the H_2 content in $R_{Control}$ dropped quickly to a low level by day 8, which was critical to pull the oxidation of HPr (Meng et al., 2013). In short, despite the positive role of ZVI and LZVI in avoiding the accumulation of HPr at the initial stage of AD, the advantage did not last long. Under stress-free environment, $R_{Control}$ quickly adjusted itself to achieve process stability. This might partly explain the insignificant improvement effect of ZVI and LZVI on the AD performance in the present work.

The variations of soluble organic products during AD at high ammonia stress are shown in Figure S3 (Supplementary data). As illustrated in Figure S3(a), the addition of 5 g/L ZVI/LZVI contributed to a lower level of sCOD in relative to $R'_{Control}$, which was attributable to the promotion effect of ZVI on sCOD degradation via enhancing acidification and methanogenesis at high ammonia stress (Yang et al., 2018). A higher level of sCOD was detected in R'_{LZVI} than that in R'_{ZVI}, this could be explained by the more significant promotion effect of LZVI on hydrolysis than pristine ZVI (Feng et al., 2014). Similar to the trends of sCOD, the existence of ZVI significantly lowered the concentrations of both soluble proteins and soluble carbohydrates, while LZVI addition resulted in higher levels of these two substances (Figure S3(b) and (c)). Figure S3(d) demonstrates the concentrations of VFAs in ammonia-stressed AD reactors. Significant HPr accumulation was observed in $R'_{Control}$ during day 4–16, while a much lower level of HPr was achieved with ZVI/LZVI, this was in accordance with Yang et al. (2018), who suggested that ZVI could facilitate HPr conversion to overcome ammonia inhibition.

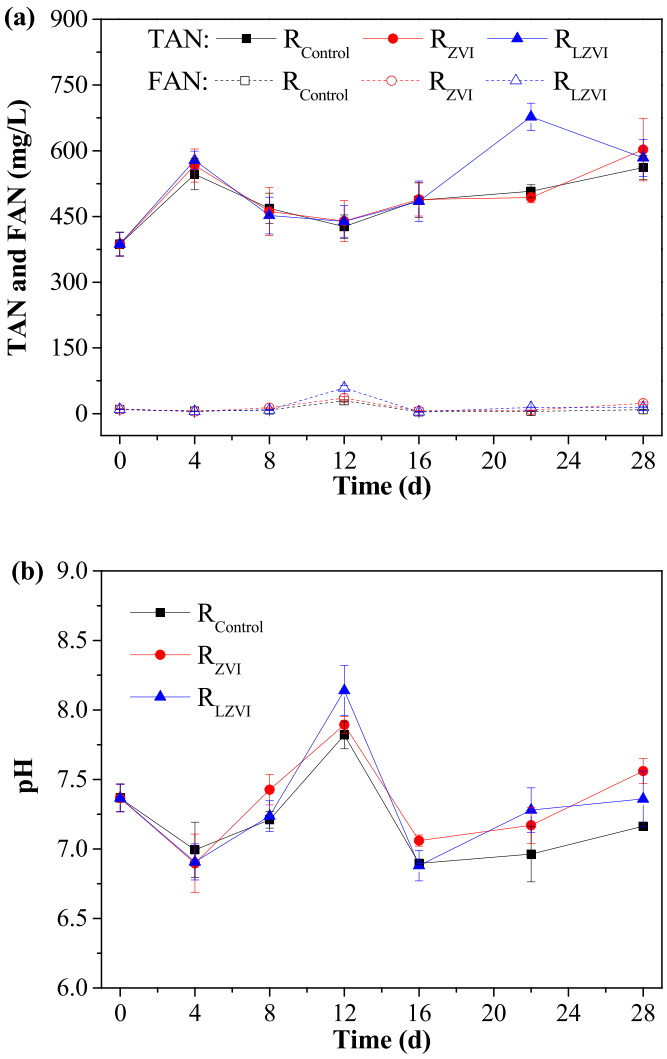

Fig. 3. Changes of (a) TAN/FAN and (b) system pH during AD at stress-free environment.

3.3. Ammonia and pH

It can be seen from Fig. 3(a) that the concentrations of TAN in $R_{Control}$, R_{ZVI} and R_{LZVI} fluctuated between 387.0 and 677.5 mg/L during the 28 days' fermentation. And the concentrations of FAN varied within a range of 4.1–58.9 mg/L. Both TAN and FAN concentrations in the three reactors were much lower than the inhibition threshold values reported

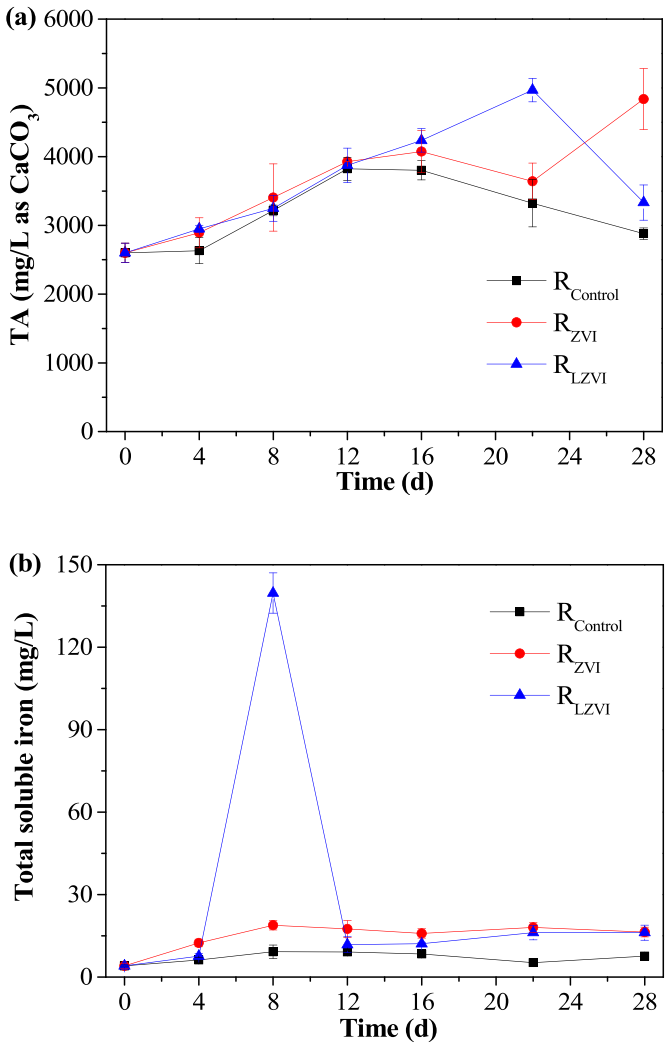

Fig. 4. Profiles of (a) TA and (b) total soluble iron during AD at stress-free environment.

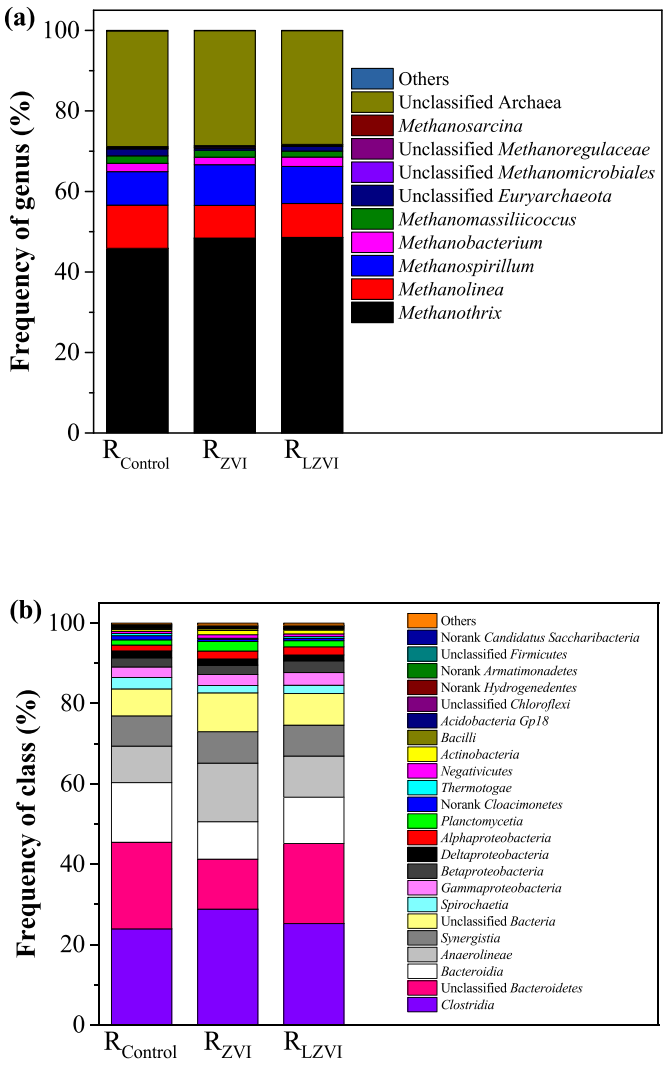

Fig. 5. Relative abundances of the (a) archaeal populations in genus level and (b) bacterial populations in class level.

in the literatures (Rajagopal et al., 2013; Jiang et al., 2019; Yu et al., 2020). As shown in Fig. 3(b), the pH variation trends in the three reactors were quite similar, hit the top at around 8.0 on day 12, followed by a decrease to around 7.0 on day 16, and finally increased to 7.2 ($R_{Control}$), 7.6 (R_{ZVI}) and 7.4 (R_{LZVI}), respectively. The addition of ZVI/LZVI slightly raised the system pH as a result of hydrogen evolution corrosion (Wei et al., 2018). For all reactors, the pH fluctuated within a weakly alkaline range of 6.9–8.1, which were very suitable for AD of SM (Mao et al., 2017). The above results confirmed that the digesters were operated at a non-hostile environment.

The changes in ammonia concentration and system pH in $R'_{Control}$, R'_{ZVI} and R'_{LZVI} are shown in Figure S4(a) and (b) (Supplementary data), respectively. Significantly higher levels of FAN were observed from these reactors (39.8–101.6 mg/L), when being compared with those operated under stress-free environment (4.1–58.9 mg/L). It was noticeable that the level of TAN in R'_{LZVI} was significantly higher than those in R'_{ZVI} and $R'_{Control}$, this phenomenon might be explained by the great promotion effects of LZVI on both hydrolysis and acidification. The pH fluctuated within a range of 7.0–7.4. This range was lower than those in digesters operated at stress-free environment (7.0–8.1), and the phenomenon could be explained by the accumulation of VFAs as a result of ammonia inhibition (Rajagopal et al., 2013).

3.4. Total alkalinity and total soluble iron

As illustrated in Fig. 4(a), the concentrations of TA in $R_{Control}$, R_{ZVI} and R_{LZVI} varied within a range of 2599.9–4968.4 mg/L as $CaCO_3$. And the TA concentration in $R_{Control}$ was lower than that in R_{ZVI} or R_{LZVI}, which was in accordance with the previous study conducted by Kong et al. (2016), who indicated that ZVI dissolution could increase the TA concentration and improve the system buffering capacity to prevent excess acidification.

Generally, the physicochemical and biochemical reactions of ZVI during AD process are: 1) Fe^0 loses electrons to generate Fe^{2+}; 2) Fe^{2+} reacts with OH^-, S^{2-}, PO_4^{3-} or other ions to form precipitates; 3) as an essential element of many anaerobic microbes, it can be utilized by microorganisms (Thanh et al., 2016). Therefore, the instantaneous concentrations of total soluble iron was influenced by the dissolution efficiency of ZVI and the precipitation rate of ferrous ions. According to Fig. 4(b), the total soluble iron in $R_{Control}$ raised slowly from 4.0 to 7.6 mg/L during the experiment. The existence of ZVI contributed to a slightly higher level of total soluble iron in R_{ZVI}, increasing gradually from 4.0 to 16.4 mg/L by the end of experiment. While a much higher level of total soluble iron was recorded in R_{LZVI}, attaining a maximum value of 139.7 mg/L (2.5 mmol/L) on day 8, which proved the much greater dissolution efficiency of LZVI than pristine ZVI. In the weakly alkaline environment during AD of SM, the iron ions would be

Table 2
Effect of ZVI addition on AD in different conditions.

Substrate	Initial AD conditions (mixture of inocula + substrate)					CH_4 production performance			Reference
	Initial TAN (mg/L)	TS (%)	F/M ratio [a] (VS based)	ZVI size (μm)	ZVI dosage (g/L)	CH_4 yield (mL/g VS_{fed})	Increase relative to control (%)	Role of ZVI	
SM [b]	387.0	7.5	3.9	1–10	5.0	135.0	0	–	This study
SM	~4000.0	10.4	2.2	1–10	5.0	60.3	11.6	Consolidate hydrogenotrophic methanogenesis pathway and relieve ammonia inhibition	This study
SM	~5000.0	10.8	4.0	0.5–10	5.0	167.9	54.2	Optimize fermentation type and provide extra H_2 for hydrogenotrophic processes	Yang et al. (2018)
SM	3178.6	12.1	6.7	~10	5.0	123.7	77.0	Provide more H_2 and electrons to facilitate H_2-utilizing processes and DIET	Huang et al. (2019b)
SM	5000.0–5500.0	10.0	4.1	150	17.9	400.6	22.2	Accelerate propionate degradation and alleviate ammonia inhibition	Meng et al. (2020)
SM	2600.0	8.0	0.8	No reported	21.0	275.0	23.9	Accelerate acetate/propionate transformation and reduce antibiotic resistance genes	Zhang et al. (2021)
FW [c]	/	10.0	2.0	2×10^2	5.6	380.0	Little CH_4 yield in control	Buffer system pH and alleviate excessive acidification	Kong et al. (2016)
FW	/	14.7	2.0	4×10^{-2}	2.0	103.7	35.4	Promote VFAs conversion, facilitate electron transfer and reduce antibiotic resistance genes	Wang et al. (2019)
FW + sludge	/	4.5	15.0	2×10^2	10.0	238.68	20	Enhance relative abundance of DIET-related microorganisms	Chen et al. (2020)
Sludge	/	15.0	/	2×10^2	17	101.0	40.8	Enhance the buffer capacity of AD system	Suanon et al. (2017)

[a] F/M ratio-food to microorganism ratio.
[b] SM-swine manure.
[c] FW-food waste.

precipitated quickly or utilized by microbes, this could be the reason why the total soluble iron in R_{LZVI} dropped sharply after day 8.

3.5. Microbial analysis

Fig. 5(a) exhibits the genus level distributions of the archaeal communities in the three reactors. Overall, no distinct difference in the archaeal community structure was observed from the three digesters. As shown, *Methanothrix* spp. was most abundant in all digesters, followed by *Methanolinea*, *Methanospirillum* and *Methanobacterium* spp. The relative abundance of *Methanothrix* spp. was determined to be 45.9% in $R_{Control}$, 48.4% in R_{ZVI} and 48.6% in R_{LZVI}, respectively. Acetoclastic *Methanothrix* spp. are featured by slow growth rate and susceptibility to inhibitors or hostile environments (Yan et al., 2020). Its dominance in the three reactors confirmed that they were running under stress-free environment. Overall, ZVI/LZVI addition didn't facilitate the growth of hydrogenotrophic methanogens or change the dominant position of acetoclastic *Methanothrix* spp. For the three reactors, the total relative abundance of hydrogenotrophic methanogens (*Methanolinea*, *Methanospirillum*, *Methanobacterium* and *Methanomassiliicoccus* spp.) in archaea varied within a narrow range of 21.5%–23.0%. Previous studies have suggested that ZVI addition in AD reactors could significantly enrich the hydrogenotrophic methanogens (Wang et al., 2019; Xu et al., 2019a; Yuan et al., 2021). Xu et al. (2019a) indicated that nZVI supplementation during AD of black water at high ammonia level could increase the gene copy concentrations assigned to hydrogenotrophic methanogens by 23.0%–108.6%. The supplementation of ZVI has been suggested to alleviate excessive acidification during AD of FW through enriching *Methanobacterium* spp., typical H_2-utilizing methanogens (Kong et al., 2016). Huang et al. (2019c) also suggested that ZVI could increase the overall abundance of hydrogenotrophic methanogens during AD of SM at a high antibiotic level of 200 mg/L, helping achieve a 36.9% greater CH_4 production efficiency and an 86.8% higher sulfadiazine removal efficiency. It was noticeable that the above studies were all performed under stressed environment, which were different from the current work. The fact that ZVI/LZVI did not significantly change the archaeal community structure might partially explain the similar CH_4 production efficiencies of the three reactors.

Fig. 5(b) demonstrates the class level distributions of bacterial communities. The top five dominant bacteria in the three reactors were *Clostridia*, unclassified *Bacteroidetes*, *Bacteroidia*, *Anaerolineae* and *Synergistia*, they were responsible for over 75% of the bacterial sequences. Compared with $R_{Control}$, ZVI addition contributed to increased relative abundances of *Clostridia* and *Anaerolineae* in R_{ZVI} by 20.5% and 59.8%, respectively. And the supplementation of LZVI contributed to increased relative abundances of these two classes in R_{LZVI} by 5.4% and 12.2%, respectively. *Clostridia* show diverse metabolic capabilities, and they cover many important species involved in HBu fermentation, syntrophic acetate oxidation and homoacetogenesis (Huang et al., 2019b). *Anaerolineae* play an essential role in the production of acetic acids (HAc), lactate and H_2 during the fermentation process (Xia et al., 2016). Their enrichment upon the supplementation of ZVI and LZVI might boost HAc/H_2 generation. Compared with the archaeal communities, ZVI and LZVI had a more significant impact on the relative abundances of certain bacterial members. But because of the faster growth and evolution of bacteria compared to methanogens (Venkiteshwaran et al., 2015), the distribution of bacterial community structure might not be a key indicator of the process performance. Xu et al. (2019b) studied the effects of antibiotic on AD performance and microbial community structures, and they reported that the distribution of archaea showed a correlative relationship with the CH_4 production performance, while the bacterial community structure was less influential.

3.6. Implications

The effects of ZVI on AD performance under different scenarios are summarized in Table 2. AD shows great potentials in recovering energy from organic solids and stabilizing the wastes, and ZVI addition has been proved to be effective in improving the methanogenesis performance under stressed/hostile environment like toxicant inhibition, excessive acidification or high solid content. However, ZVI addition is not always effective for all AD systems, especially those operated under stress-free

environment. The addition of ZVI might not be capable of improving the overall anaerobic biodegradability of all feedstocks. For digesters operating under non-hostile environment, improving the substrate biodegradability using physicochemical pretreatment methods might be a more viable option. Our future studies will focus more on the revival of process depression using ZVI, as well as the combination of ZVI with physicochemical pretreatment approaches to achieve greater organic solid removal efficiency and higher CH_4 yield.

4. Conclusions

In the healthy digesters treating SM, ZVI could neither enhance the biodegradability of SM nor change the archaeal community structure, and its improvement effect on AD performance was negligible. In this circumstance, application of physicochemical pretreatments for improving feedstock biodegradability is more practical. Under stressed environment, ZVI could alter the metabolism pathways and enhance the microbial activity to alleviate process depression, and liquid nitrogen pretreatment could greatly accelerate the dissolution of ZVI and strengthen its enhancement effect on AD performance. To realize ZVI's full potential in enhancing CH_4 yield from organic manure, future efforts shall be made to study the reversibility of process inhibition.

Author contributions statement

Ziyin Ai: Investigation, Writing – original draft. **Sichao Zheng**: Investigation. **Dan Liu**: Investigation. **Siyuan Wang**: Data curation. **Hongqin Wang**: Methodology. **Wenli Huang**: Validation. **Zhongfang Lei**: Conceptualization. **Zhenya Zhang**: Visualization. **Fei Yang**: Supervision. **Weiwei Huang**: Writing – review & editing, Funding acquisition.

Declaration of competing interest

The authors declare that they have no known competing financial interests or personal relationships that could have appeared to influence the work reported in this paper.

Data availability

No data was used for the research described in the article.

Acknowledgements

This work was financially supported by Hainan Provincial Natural Science Foundation of China (420RC531), National Natural Science Foundation of China (52060005), Tianjin University- Hainan University Innovation Funding and Research Foundation of Hainan University (KYQD (2R) 1930).

Appendix A. Supplementary data

Supplementary data to this article can be found online at https://doi.org/10.1016/j.chemosphere.2022.135544.

References

APHA, 2012. Standard Methods for the Examination of Water and Wastewater, twenty-second ed. American Public Health Association (APHA), American Water Works Association (AWWA) and Water Environment Federation (WEF), Washington, D.C., USA.

Cao, Y., Chang, Z., Wang, J., Ma, Y., Fu, G., 2013. The fate of antagonistic microorganisms and antimicrobial substances during anaerobic digestion of pig and dairy manure. Bioresour. Technol. 136, 664–671. https://doi.org/10.1016/j.biortech.2013.01.052.

Cazier, E.A., Trably, E., Steyer, J.P., Escudie, R., 2019. Reversibility of hydrolysis inhibition at high hydrogen partial pressure in dry anaerobic digestion processes fed with wheat straw and inoculated with anaerobic granular sludge. Waste Manage. (Tucson, Ariz.) 85, 498–505. https://doi.org/10.1016/j.wasman.2019.01.019.

Charalambous, P., Vyrides, I., 2021. In situ biogas upgrading and enhancement of anaerobic digestion of cheese whey by addition of scrap or powder zero-valent iron (ZVI). J. Environ. Manag. 280, 111651 https://doi.org/10.1016/j.jenvman.2020.111651.

Chen, S., Tao, Z., Yao, F., Wu, B., He, L., Hou, K., Pi, Z., Fu, J., Yin, H., Huang, Q., Liu, Y., Wang, D., Li, X., Yang, Q., 2020. Enhanced anaerobic co-digestion of waste activated sludge and food waste by sulfidated microscale zerovalent iron: insights in direct interspecies electron transfer mechanism. Bioresour. Technol. 316, 123901 https://doi.org/10.1016/j.biortech.2020.123901.

Dubois, M., Gilles, K.A., Hamilton, J.K., Rebers, P.A., Smith, F., 1956. Colorimetric method for determination of sugars and related substances. Anal. Chem. 28, 350–356.

Fan, P., Li, L., Sun, Y., Qiao, J., Xu, C., Guan, X., 2019. Selenate removal by Fe^0 coupled with ferrous iron, hydrogen peroxide, sulfidation, and weak magnetic field: a comparative study. Water Res. 159, 375–384. https://doi.org/10.1016/j.watres.2019.05.037.

Feng, Y., Zhang, Y., Quan, X., Chen, S., 2014. Enhanced anaerobic digestion of waste activated sludge digestion by the addition of zero valent iron. Water Res. 52, 242–250. https://doi.org/10.1016/j.watres.2013.10.072.

Guan, X., Sun, Y., Qin, H., Li, J., Lo, I.M.C., He, D., Dong, H., 2015. The limitations of applying zero-valent iron technology in contaminants sequestration and the corresponding countermeasures: the development in zero-valent iron technology in the last two decades (1994-2014). Water Res. 75, 224–248. https://doi.org/10.1016/j.watres.2015.02.034.

Hu, Y., Peng, X., Ai, Z., Jia, F., Zhang, L., 2019. Liquid nitrogen activation of zero-valent iron and its enhanced Cr (VI) removal performance. Environ. Sci. Technol. 53, 8333–8341. https://doi.org/10.1021/acs.est.9b01999.

Hu, Y., Zang, Y., Yang, Y., Duan, A., Wang, X.C., Ngo, H.H., Li, Y., Du, R., 2020. Zero-valent iron addition in anaerobic dynamic membrane bioreactors for preconcentrated wastewater treatment: performance and impact. Sci. Total Environ. 742, 140687 https://doi.org/10.1016/j.scitotenv.2020.140687.

Huang, H., He, L., Zhang, Z., Lei, Z., Liu, R., Zheng, W., 2019a. Enhanced biogasification from ammonia-rich swine manure pretreated by ammonia fermentation and air stripping. Int. Biodeterior. Biodegrad. 140, 84–89. https://doi.org/10.1016/j.ibiod.2019.03.014.

Huang, W., Yang, F., Huang, W., Wang, D., Lei, Z., Zhang, Z., 2019b. Weak magnetic field significantly enhances methane production from a digester supplemented with zero valent iron. Bioresour. Technol. 282, 202–210. https://doi.org/10.1016/j.biortech.2019.03.013.

Huang, W., Yang, F., Huang, W., Lei, Z., Zhang, Z., 2019c. Enhancing hydrogenotrophic activities by zero-valent iron addition as an effective method to improve sulfadiazine removal during anaerobic digestion of swine manure. Bioresour. Technol. 294, 122178 https://doi.org/10.1016/j.biortech.2019.122178.

Inaba, R., Nagoya, M., Kouzuma, A., Watanabe, K., 2019. Metatranscriptomic evidence for magnetite nanoparticle-stimulated acetoclastic methanogenesis under continuous agitation. Appl. Environ. Microbiol. 85, e01733-19 https://doi.org/10.1128/AEM.01733-19.

Jiang, C., Wu, Z., Li, R., Liu, Q., 2011. Technology of protein separation from whey wastewater by two-stage foam separation. Biochem. Eng. J. 55, 43–48. https://doi.org/10.1016/j.bej.2011.03.005.

Jiang, Y., McAdam, E., Zhang, Y., Heaven, S., Banks, C., Longhurst, P., 2019. Ammonia inhibition and toxicity in anaerobic digestion: a critical review. J. Water Proc. Eng. 32, 100899 https://doi.org/10.1016/j.jwpe.2019.100899.

Kong, X., Wei, Y., Xu, S., Liu, J., Li, H., Liu, Y., Yu, S., 2016. Inhibiting excessive acidification using zero-valent iron in anaerobic digestion of food waste at high organic load rates. Bioresour. Technol. 211, 65–71. https://doi.org/10.1016/j.biortech.2016.03.078.

Kong, X., Niu, J., Zhang, W., Liu, J., Yuan, J., Li, H., Yue, X., 2021. Mini art review for zero valent iron application in anaerobic digestion and technical bottlenecks. Sci. Total Environ. 791, 148415 https://doi.org/10.1016/j.scitotenv.2021.148415.

Li, L., Xu, Y., Dai, X., Dai, L., 2021. Principles and advancements in improving anaerobic digestion of organic waste via direct interspecies electron transfer. Renew. Sustain. Energy Rev. 148, 111367 https://doi.org/10.1016/j.rser.2021.111367.

Mao, C., Wang, X., Xi, J., Feng, Y., Ren, G., 2017. Linkage of kinetic parameters with process parameters and operational conditions during anaerobic digestion. Energy 135, 352–360. https://doi.org/10.1016/j.energy.2017.06.050.

Meng, X., Zhang, Y., Li, Q., Quan, X., 2013. Adding Fe^0 powder to enhance the anaerobic conversion of propionate to acetate. Biochem. Eng. J. 73, 80–85. https://doi.org/10.1016/j.bej.2013.02.004.

Meng, X., Sui, Q., Liu, J., Yu, D., Wang, Y., Wei, Y., 2020. Relieving ammonia inhibition by zero-valent iron (ZVI) dosing to enhance methanogenesis in the high solid anaerobic digestion of swine manure. Waste Manage. (Tucson, Ariz.) 118, 452–462. https://doi.org/10.1016/j.wasman.2020.08.021.

Pan, X., Lv, N., Cai, G., Zhou, M., Wang, R., Li, C., Ning, J., Li, Y., Ye, Z., Zhu, G., 2021. Carbon- and metal-based mediators modulate anaerobic methanogenesis and phenol removal: focusing on stimulatory and inhibitory mechanism. J. Hazard Mater. 420, 126615 https://doi.org/10.1016/j.jhazmat.2021.126615.

Rajagopal, R., Massé, D., Singh, G., 2013. A critical review on inhibition of anaerobic digestion process by excess ammonia. Bioresour. Technol. 143, 632–641. https://doi.org/10.1016/j.biortech.2013.06.030.

Rezaei, F., Vione, D., 2018. Effect of pH on zero valent iron performance in heterogeneous Fenton and Fenton-like processes: a review. Molecules 23, 3127. https://doi.org/10.3390/molecules23123127.

Shao, Z., Guo, X., Qu, Q., Kang, K., Su, Q., Wang, C., Qiu, L., 2021. Effects of chlorine disinfectants on the microbial community structure and the performance of anaerobic digestion of swine manure. Bioresour. Technol. 339, 125576 https://doi.org/10.1016/j.biortech.2021.125576.

Suanon, F., Sun, Q., Li, M., Cai, X., Zhang, Y., Yan, Y., Yu, C., 2017. Application of nanoscale zero valent iron and iron powder during sludge anaerobic digestion: impact on methane yield and pharmaceutical and personal care products degradation. J. Hazard Mater. 321, 47–53. https://doi.org/10.1016/j.jhazmat.2016.08.076.

Summer, D., Schöftner, P., Watzinger, A., Reichenauer, T.G., 2020. Inhibition and stimulation of two perchloroethene degrading bacterial cultures by nano- and micro-scaled zero-valent iron particles. Sci. Total Environ. 722, 137802 https://doi.org/10.1016/j.scitotenv.2020.137802.

Tang, C., Huang, Y., Zhang, Z., Chen, J., Zeng, H., Huang, Y.H., 2016. Rapid removal of selenate in a zero-valent iron/Fe_3O_4/Fe^{2+} synergetic system. Appl. Catal., B 184, 320–327. https://doi.org/10.1016/j.apcatb.2015.11.045.

Tang, H., Holmes, D.E., Ueki, T., Palacios, P.A., Lovley, D.R., 2019. Iron corrosion via direct metal-microbe electron transfer. mBio 10, e00303–e00319. https://doi.org/10.1128/mBio.00303-19.

Thanh, P.M., Ketheesan, B., Yan, Z., Stuckey, D., 2016. Trace metal speciation and bioavailability in anaerobic digestion: a review. Biotechnol. Adv. 34, 122–136. https://doi.org/10.1016/j.biotechadv.2015.12.006.

Venkiteshwaran, K., Bocher, B., Maki, J., Zitomer, D., 2015. Relating anaerobic digestion microbial community and process function. Microbiol. Insights 8, 37–44. https://doi.org/10.4137/MBI.S33593.

Wang, P., Chen, X., Liang, X., Cheng, M., Ren, L., 2019. Effects of nanoscale zero-valent iron on the performance and the fate of antibiotic resistance genes during thermophilic and mesophilic anaerobic digestion of food waste. Bioresour. Technol. 293, 122092 https://doi.org/10.1016/j.biortech.2019.122092.

Wang, X., Lyu, T., Dong, R., Liu, H., Wu, S., 2021. Dynamic evolution of humic acids during anaerobic digestion: exploring an effective auxiliary agent for heavy metal remediation. Bioresour. Technol. 320, 124331 https://doi.org/10.1016/j.biortech.2020.124331.

Wei, J., Hao, X., Van Loosdrecht, M.C.M., Li, J., 2018. Feasibility analysis of anaerobic digestion of excess sludge enhanced by iron: a review. Renew. Sustain. Energy Rev. 89, 16–26. https://doi.org/10.1016/j.rser.2018.02.042.

Wu, D., Zheng, S., Ding, A., Sun, G., Yang, M., 2015. Performance of a zero valent iron-based anaerobic system in swine wastewater treatment. J. Hazard Mater. 286, 1–6. https://doi.org/10.1016/j.jhazmat.2014.12.029.

Xia, Y., Wang, Y., Wang, Y., Chin, F.Y.L., Zhang, T., 2016. Cellular adhesiveness and cellulolytic capacity in *Anaerolineae* revealed by omics-based genome interpretation. Biotechnol. Biofuels 9, 111. https://doi.org/10.1186/s13068-016-0524-z.

Xu, R., Xu, S., Zhang, L., Florentino, A.P., Yang, Z., Liu, Y., 2019a. Impact of zero valent iron on blackwater anaerobic digestion. Bioresour. Technol. 285, 121351 https://doi.org/10.1016/j.biortech.2019.121351.

Xu, R., Yang, Z., Zheng, Y., Wang, Q., Bai, Y., Liu, J., Zhang, Y., Xiong, W., Lu, Y., Fan, C., 2019b. Metagenomic analysis reveals the effects of long-term antibiotic pressure on sludge anaerobic digestion and antimicrobial resistance risk. Bioresour. Technol. 282, 179–188. https://doi.org/10.1016/j.biortech.2019.02.120.

Yan, W., Mukherjee, M., Zhou, Y., 2020. Direct interspecies electron transfer (DIET) can be suppressed under ammonia-stressed condition - reevaluate the role of conductive materials. Water Res. 183, 116094 https://doi.org/10.1016/j.watres.2020.116094.

Yang, Y., Yang, F., Huang, W., Huang, W., Li, F., Lei, Z., Zhang, Z., 2018. Enhanced anaerobic digestion of ammonia-rich swine manure by zero-valent iron: with special focus on the enhancement effect on hydrogenotrophic methanogenesis activity. Bioresour. Technol. 270, 172–179. https://doi.org/10.1016/j.biortech.2018.09.008.

Yu, D., Zhang, J., Chulu, B., Yang, M., Nopens, I., Wei, Y., 2020. Ammonia stress decreased biomarker genes of acetoclastic methanogenesis and second peak of production rates during anaerobic digestion of swine manure. Bioresour. Technol. 317, 124012 https://doi.org/10.1016/j.biortech.2020.124012.

Yuan, T., Shi, X., Sun, R., Ko, J.H., Xu, Q., 2021. Simultaneous addition of biochar and zero-valent iron to improve food waste anaerobic digestion. J. Clean. Prod. 278, 123627 https://doi.org/10.1016/j.jclepro.2020.123627.

Zhang, J., Lu, T., Zhong, H., Shen, P., Wei, Y., 2021. Zero valent iron improved methane production and specifically reduced aminoglycoside and tetracycline resistance genes in anaerobic digestion. Waste Manage. (Tucson, Ariz.) 136, 122–131. https://doi.org/10.1016/j.wasman.2021.10.010.

Zheng, S., Yang, F., Huang, W., Lei, Z., Zhang, Z., Huang, W., 2022. Combined effect of zero valent iron and magnetite on semi-dry anaerobic digestion of swine manure. Bioresour. Technol. 346, 126438 https://doi.org/10.1016/j.biortech.2021.126438.